LITHIUM INSERTION INTO β–MnO$_2$ AND THE RUTILE-SPINEL TRANSFORMATION

W.I.F.David*, M.M.Thackeray+, P.G.Bruce, and J.B.Goodenough
Inorganic Chemistry Laboratory, South Parks Road,
University of Oxford, Oxford OX1 3QR
England

ABSTRACT
Room-temperature lithium insertion with n-butyl lithium into the
rutile phase β–MnO$_2$ results in a product Li$_{1-\delta}$MnO$_2$ that is shown to
be isostructural with the tetragonal Li$_2$[Mn$_2$]O$_4$ phase obtained by
room-temperature lithiation of the spinel Li[Mn$_2$]O$_4$; it is
distinguishable from the orthorhombic LiMnO$_2$ phase obtained with
high-temperature synthesis, contrary to a previous report on
lithiated β–MnO$_2$. A model of the transformation mechanism, on
lithiation, from the β–MnO$_2$ framework to the [Mn$_2$]O$_4$ framework of a
spinel phase is suggested.

Introduction

Topochemical reactions with lithium have both a technical and a scientific
importance. Technically, reversible lithium insertion into oxides and
sulfides is of interest for electrodes in both electrochromic displays [1]
and secondary batteries [2]. Scientifically, room-temperature lithium
insertion and/or extraction, either chemically or electrochemically,
provides a synthetic route to unusual products [3,4] and unusual atomic
order [5].

Two-dimensional (2D) insertion of lithium into the layered oxides V$_2$O$_5$[6]
and MoO$_3$[7] has been demonstrated; 2D extraction of lithium from the
layered oxides LiMO$_2$, M = Cr, Co or Ni, gives rise to

* Present Address: SERC Rutherford-Appleton Laboratory, Chilton,
        Didcot OX11 OQX, UK.
+ Present Address: National Physical Research Laboratory CSIR,
        PO Box 395, Pretoria 0001, South Africa.

atmospheric-pressure preparation of oxides with cations of high valence
state [4]. Murphy et al [8] have studied 1D lithiation of several rutile
phases MO_2, including $\beta-MnO_2$, and we [5,9] have reported the
room-temperature 3D lithiation of several spinels: cubic Fe_3O_4 and
$Li[Mn_2]O_4$ to obtain $Li_xFe_3O_4$ with $0<x<2$ and $Li_{1+x}[Mn_2]O_4$ with $0<x\leqslant1$,
tetragonal Mn_3O_4 to obtain tetragonal $Li_xMn_3O_4$ with $0<x<1$.
Transformation of the anatase phase of TiO_2 to the spinel $Li[Ti_2]O_4$ on
lithiation has also been reported [10].

In this paper, we re-examine the product of room-temperture, chemical
lithiation of the rutile phase $\beta-MnO_2$ because of the importance of
activated $\gamma-MnO_2$ as a cathode material in several lithium-based primary
cells. The activated $\gamma-MnO_2$ phase consists of a ramsdellite matrix with
intergrowth domains of $\beta-MnO_2$[11]. Little information is available on the
structural changes that occur upon lithium insertion into the
electroactive material. However, a recent study of the lithiation of
$\beta-MnO_2$[8] has indicated that up to 0.3 lithium atoms per formula unit may
be topochemically inserted into the structure without transforming the
rutile framework; on further lithiation the product is reported to become
the orthorhombic $LiMnO_2$ phase obtained directly from high-temperature
synthesis. The orthorhombic $LiMnO_2$ phase has Li^+ and Mn^{3+} ions ordered
into layers of octahedral sites, thus providing only a 2D interstitial
space for Li^+-ion motion [12]. Although we were able to confirm a
disruption of the rutile framework at higher lithium concentrations, our
lithiated product had an $[Mn_2]O_4$ framework of an $A[B_2]O_4$ tetragonal spinel
with Li^+ ions occupying both octahedral and tetrahedral sites of a 3D
interstitial space. A cooperative Jahn-Teller distortion of the $[Mn_2]O_4$
framework to tetragonal (c/a>1) symmetry is induced by the octahedral-site
Mn^{3+} ions.

Experimental


Lithiation of $\beta-MnO_2$ (Koch-Light 99.95%) was carried out chemically on a
fine powder immersed in a 1.6 molar solution of n-butyl lithium in hexane
that was further diluted with sodium-dried hexane. The reagents were
stirred for approximately 170 hours at 50-60^{0}C under a dry dinitrogen
atmosphere. The product was repeatedly washed in hexane and finally dried
for several hours under vacuum.

Chemical analysis of the lithiated product was carried out by
atomic-absorption spectroscopy, which indicated a final composition of
$Li_{1\pm0.1}MnO_2$.

Structural characterization was carried out by powder X-ray diffraction on a
Philips PW1050 diffractometer with CuKα radiation and a quartz analyzing
monochromater.

Results and Discussion

The rutile structure of β-MnO_2 possesses the tetragonal space group $P4_2/mnm$ with octahedral site Mn^{4+} ions at positions 2a and O^{2-} ions at positions 4f. The 4f coordinates x,x,0; $\bar{x},\bar{x},0$; $\frac{1}{2}+x,\frac{1}{2}-x,\frac{1}{2}$; $\frac{1}{2}-x,\frac{1}{2}+x,\frac{1}{2}$ contain the variable positional parameter x, which permits distortion of the occupied octahedral sites to orthorhombic point symmetry.

c-axis

$\bullet$ - Mn^{4+}

(a) $\bigcirc$ - O^{2-} (b)
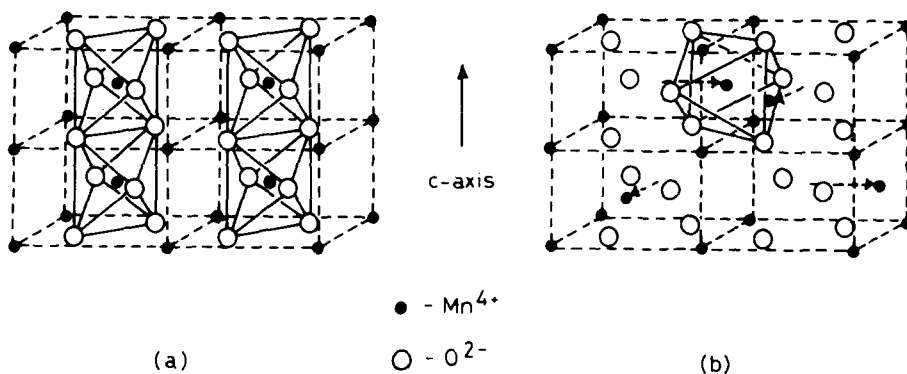
FIG. 1

(a) The rutile structure of β-MnO_2 (b) Displacement of the body-centered cations to the midpoints of the 100 and 010 unit cell faces

As illustrated in Fig. 1(a), the rutile structure consists of strings of cation-occupied, edge-shared anion octahedra parallel to the tetragonal c-axis; each string shares octahedral-site corners with four neighboring strings to give a body-centered-tetragonal cation array. The positional parameter x allows the bridging anions of a chain to approach each other so as to screen better the intrachain electrostatic repulsion between cations. The bridging Mn–O distances within a chain are shorter than the apical Mn–O distances within the basal planes.

Of particular interest is the primitive-tetragonal packing of the rutile anion array [13-15] which is derived from hexagonal close packing by cooperative rotations of the strings of corner-shared octahedra. The curved arrows of Fig. 2(a) indicate the sense of rotation of these strings that is required to restore the hexagonal close packing of the anion array illustrated in Fig. 2(b). Primitive tetragonal packing opens up the interstitial 1D channels of face-shared octahedra and tetrahedra to give them a square cross-section in the basal plane, see Fig. 2(a), and thus to optimize the possibility of 1D H^+-ion or Li^+-ion mobility within a channel parallel to the c-axis.
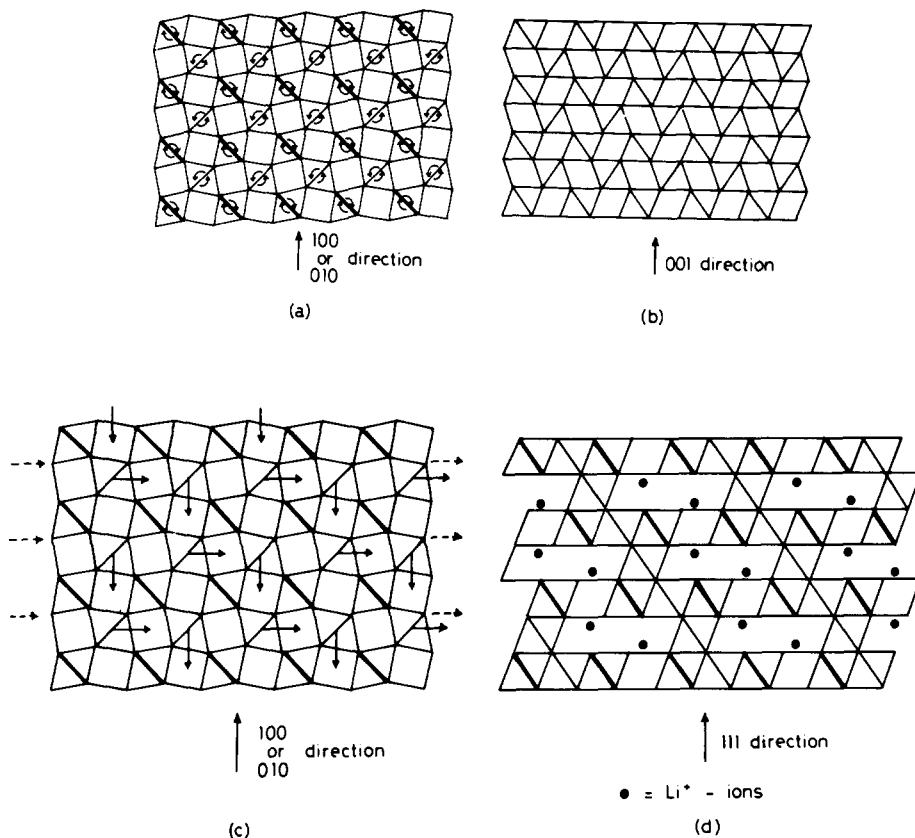
FIG. 2

Projection of (a) rutile, down the unique c-axis (b)
hexagonal-close-packed anion array derived from rutile (c) rutile and
(d) Li[Mn$_2$]O$_4$ spinel. Curved arrows in (a) indicate rotations to
(b), straight arrows in (c) indicate cation displacements to reach
(d), broken arrows in (c) indicate shear direction, ◁ , ◸ —MnO$_6$
octahedra

The X-ray-diffraction profiles of β-MnO$_2$ and of the lithiated product
L$_{1-\delta}$MnO$_2$ are shown in Fig. 3. Traces of unreacted β-MnO$_2$ are visible in
Fig. 3(b). Subtraction of the β-MnO$_2$ trace leaves a profile similar to that
of the tetragonal Li$_2$[Mn$_2$]O$_4$ phase obtained by lithiation of the spinel
Li[Mn$_2$]O$_4$ [9]. Note in particular the strong (111) peak, which is indicative
of the [Mn$_2$]O$_4$ framework of the Li[Mn$_2$]O$_4$ spinel. The significant line
broadening is due to the small particle size of the lithiated powder.

In the cubic spinel Li[Mn^{3+}Mn^{4+}]O$_4$, the cubic-close-packed oxide ions occupy
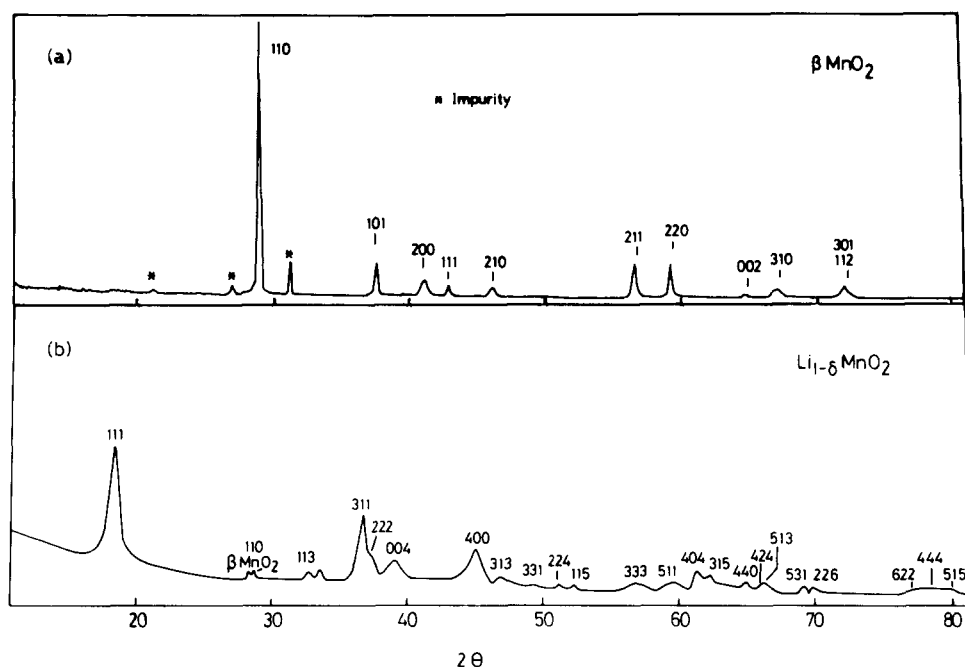positions 32e of space group Fd3m, the manganese ions occupy the half of the

FIG. 3

X-ray-diffraction powder profiles of (a) β-MnO$_2$ and (b) the lithiated product $Li_{1-\delta}MnO_2$ indexed in the face-centered tetragonal space group $F4_1/ddm$

octahedral sites designated 16d, and the Li$^+$ ions occupy the one-eighth of the tetrahedral sites designated 8a, which share faces with the empty 16c octahedral sites. The 16c sites form an array similar to the 16d-site array, but displaced half a lattice parameter along any cube axis. The remaining empty sites are the 8b tetrahedral sites sharing faces with the filled 16d sites and the 48f tetrahedral sites sharing two 16d-site and two 16c-site faces. The electrostatic forces between lithium and manganese ions in the lithiated product $Li_{1+x}[Mn_2]O_4$ favor Li$^+$-ion occupancy of 16c and 8a sites.

Room-temperature lithiation of the spinel $Li[Mn_2]O_4$ has been shown [9] to produce a phase $Li_2[Mn_2]O_4$ having the $[Mn_2]O_4$ framework of the original spinel, but distorted from cubic to tetragonal (c/a=1.16) symmetry by a cooperative Jahn-Teller distortion associated with the Mn^{3+} ions. For convenience and clarity, we refer the atomic positions in the tetragonal phase to the cubic space group Fd3m: one Li$^+$ ion per formula unit appears to occupy the tetrahedral 8a sites, as in the original spinel, and the inserted Li$^+$ ions are randomly distributed on half the 16c sites, which share faces with Li$^+$ ions on 8a sites. Although the Li$^+$-Li$^+$ electrostatic repulsions were expected to stabilize all the Li$^+$ ions on 16c positions, refinement of the powder data favored a Li$^+$-ion distribution over both 8a and 16c positions [9]. The interstitial space of face-shared 8a and 16c sites is thus only two-thirds filled, and all the 16d manganese are reduced to Mn^{3+} ions.

The structure of $Li_{1-\delta}MnO_2$ obtained from lithiated β-MnO_2 was refined, with an available program [16] from the integrated Bragg intensities of the diffraction profile of Fig. 3(b); 19 intensities from 46 reflections were used. Of the several structural models considered within the tetragonal-spinel space groups $I4_1/amd$ of $Li_2[Mn_2]O_4$, axial ratio $c/a = 1.145$, the best fit was obtained with the Li^+ ions distributed half on 8a sites and half randomly distributed on 16c sites as in the $Li_2[Mn_2]O_4$ phase obtained by lithiating $Li[Mn_2]O_4$. Refined structural parameters for this model are given in Table 1; the reliability factor $R = 100 \sum |Iobs-Icalc|/\sum Iobs = 16.0$ percent was obtained with isotropic temperature factors for the O^{2-} and Mn^{3+} ions. Although it is impossible to determine Li^+-ion occupancies accurately because of the weak scattering power of this ion, it is clear from Table 1 that significant Li^+-ion concentrations are to be found on both the 8a and 16c positions of the cubic-spinel space group. Furthermore, the magnitude of the c/a ratio is consistent with a nearly complete reduction of all the 16d octahedral-site manganese to the Mn^{3+} state. Therefore we may conclude that the phase we obtained from low-temperature chemical lithiation of the rutile phase β-MnO_2 is the tetragonal spinel-related phase $(Li_{1-\delta})_{16c}Li_{8a}[Mn_2^{3+}]_{16d}O_4$.

The orthorhombic $LiMnO_2$ phase obtained by high-temperature synthesis has a different ordering of Mn^{3+} ions on the octahedral sites of the distorted cubic-close-packed anion array. Alternate layers of manganese and lithium produce a unique axis that is not coincident with the unique axis generated by a cooperative Jahn-Teller distortion of the Mn^{3+} ions, so the net symmetry is orthorhombic [12].

TABLE 1

Structural Parameters of $Li_{1-\delta}MnO_2$, R=16.0%

Space Group $I4_1/amd$ (D_{4h}^{19}); a=5.672, c=9.182

Ion	Position*	x	y	z	Biso	occupancy
Li^+	8a	0	0.75	0.125	1	1.0
Li^+	16c	0	0	0	1	1.0
Mn^{3+}	16d	0	0	0.5	0.4(5)	0.97(6)
O^{2-}	32e	0	0.505(3)	0.277(7)	4(3)	1.0

* Positions refer to the cubic spinel space group, Fd3m.

The Rutile-Spinel Transformation

As shown in Fig. 2, the rutile-spinel transformation is essentially diffusionless and only a little more complicated than the change from primitive-tetragonal to hexagonal close packing of the anions. The latter change only requires the rotation of edge-shared strings of octahedra, shown in Fig. 2(a) by the curved arrows, to generate the hexagonal configuration of Fig. 2(b). The rutile-spinel transformation on the other hand, requires a cooperative jump to a nearest-neighbor site of half the cation array followed by an adjustment of the Mn-O distances to convert the tetragonal anion packing of rutile to the cubic close packing of anions in spinel.

Cations in half the c-axis chains remain fixed. Alternate cations in the
remaining, body-centered, c-axis chains are displaced to distorted octahedral
sites at the mid-points of the 100 unit-cell faces Fig.1(b). The remaining
cations in the chains are similarly displaced to octahedral sites at the
mid-points of the 010 unit-cell faces. This results in a redistribution of
the cations between the tetagonally packed oxide layers as shown by the arrows
in Fig. 2(c). A diffusionless readjustment of the anion array to give regular
octahedra about the manganese but without shared faces, gives the $[Mn_2]O_4$
spinel framework shown in Fig. 2(d). These adjustments can be made by a shear
motion, represented by the arrows at the side of Fig. 2(c), that flops the
distorted octahedra of the square channels in a direction opposite to the
curved arrows of Fig. 2(a).

The driving force for the rutile-spinel transformation is the electrostatic
repulsion between Li^+ and $Mn^{4+/3+}$ ions. The initial lithium atoms enter the
square channels of the rutile phase as Li^+ ions; they donate one electron each
to the manganese array to reduce Mn^{4+} to Mn^{3+}. Within a square channel, a Li^+
ion shares site faces with two neighboring manganese ions; and transformation
to hexagonal close packing of the anions would only increase this
electrostatic repulsion. Therefore we must expect a transformation to a
cubic close packing of the anions in which octahedral sites share only edges.

The spinel framework is seen to be directly accessible from the rutile
structure via an essentially diffusionless transition. Room-temperature
rearrangement of the Li^+ ions to optimal interstitial positions confronts no
significant diffusional barrier. We presume that the energy difference
between the manganese ordering in the orthorhombic $LiMnO_2$ phase and in the
$[Mn_2]O_4$ spinel framework is small and the spinel framework may be the more
stable if the phase is Li^+-ion deficient.

Finally, a similar transformation to that described herein may occur on deep
discharge in the commercial $\gamma-MnO_2$ cathode material, which contains some
$\beta-MnO_2$.

References

1.   M.Green, Thin Solid Films 38, 89 (1976)
2.   M.S.Whittingham, Prog. Solid State Chem., 12, 41 (1978)
3.   R.Schöllhorn, Angewandte Chemie, 19, 983 (1980)
4.   K.Mizushima, P.C.Jones, P.J.Wiseman and J.B.Goodenough,
      Mater. Res. Bull., 15, 783 (1980)
5.   M.M.Thackeray, W.I.F.David and J.B.Goodenough, Mater.
      Res. Bull., 17, 785 (1982)
6.   N.Kumagai, K.Tanno, T.Nakajima and N.Watanabe,
      Electrochemica Acta, 28, 17 (1983)

7.   P.H.Christian, J.N.Carides, F.J.DiSalvo and J.V.Waszczak,
      J. Electrochem. Soc., $\underline{127}$, 2315 (1980)
8.   D.W.Murphy, F.J.DiSalvo, J.N.Carides and J.V.Waszczak,
      Mater. Res. Bull., $\underline{13}$, 1395 (1978)
9.   M.M.Thackeray, W.I.F.David, P.G.Bruce, and J.B.Goodenough,
      Mater. Res. Bull., $\underline{18}$, 461 (1983)
10.   D.W.Murphy, M.Greenblatt, S.M.Zahivrak, R.J.Cava,
      J.V.Waszczak, G.W.Hull, and R.S.Hutton, Résume de Chimie
      minérale, $\underline{19}$, 441 (1982)
11.   G.Pistoia, J. Electrochem. Soc., $\underline{129}$, 1861 (1982)
12.   R.Huppe, G.Brachtel and M.Jansen, Z. anorg, allgem. Chemie
      $\underline{417}$, 1 (1975)
13.   A.R.West and P.G.Bruce, Acta Cryst, B38, 1891 (1982)
14.   W.H.Baur, Mater. Res. Bull., $\underline{16}$, 339 (1981)
15.   W.I.F.David, P.G.Bruce and J.B.Goodenough, J. Solid State
      Chemistry, (in press).
16.   P.J.Wiseman, D. Phil. Thesis (University of Oxford, 1974)